Engineering Science and Technology, an International Journal 17 (2014) 279–283

HOSTED BY

ELSEVIER

Contents lists available at ScienceDirect

Engineering Science and Technology, an International Journal

journal homepage: http://www.elsevier.com/locate/jestch

Full length article

Surface and thermal load effects on the buckling of curved nanowires

M.E. Khater [a,*], M.A. Eltaher [b,c], E. Abdel-Rahman [a], M. Yavuz [b]

[a] Dept. of Systems Design Eng., University of Waterloo, Waterloo N2L3G1, Ontario, Canada
[b] Dept. of Mechanical and Mechatronics Eng., University of Waterloo, Canada
[c] Dept. of Mechanical Design and Production, Zagazig University, Egypt

ARTICLE INFO

Article history:
Received 16 May 2014
Received in revised form
17 July 2014
Accepted 21 July 2014
Available online 16 September 2014

Keywords:
Buckling
Curved nanowires
Surface energy
Thermal load

ABSTRACT

This paper investigates the impact of surface energy and thermal loading on the static stability of nanowires. We model nanowires as curved fixed–fixed Euler-Bernoulli beams and use Gurtin-Murdoch model to represent surface energy. The model takes into account both von Kármán strain and axial strain. We derive the nanowire equilibrium equations and deploy it to investigate the buckling of nanowires. We report the wire rise, critical buckling loads, and buckled wire configurations as functions of axial load in the presence of thermal loads. We found that surface energy has significant effect on the behaviour of silicon nanowires of diameter less than 4 nm. We also found that critical buckling load increases with increase in surface tensile stress and decreases with thermal loading.

1. Introduction

Nano materials have been the interest of many researchers over the past decade due to their enhanced properties. The difference in bonding forces between atoms on the surface and those in the material bulk results in changes in surface energies, mechanical, and electrical properties. For nanostructures, the surface to volume ratio is significant which gives rise to the effects of surface energy [1,2]. This surface effect includes the effects of surface stress, oxidation layer, and surface roughness which can result in increasing the elastic modulus as much as three times as that of the material bulk [3].

It has been experimentally validated that the material size has a direct effect on its mechanical properties such as Young's modulus and flexural rigidity. He and Lilley [4,5] studied the surface effect on the elastic behaviour and the resonant frequency of bending for nanowires at different boundary conditions. Wong et al. [6] have experimentally measured the Young's modulus for silicon carbide nanorods while it was dynamically measured by Poncharal et al. [7]. Cuenot et al. [8] introduced surface stress to study the bending behaviour of nanowires. Jing et al. [3] measured the elastic properties of silver nanowires of different diameters. They found that Young's modulus decreases with increase in wire diameter, and they attributed that to the surface effect.

Classical continuum models do not take into account the effects of surface stresses and thus fail to present accurate models for such cases [2]. To account for surface energy effects, Gurtin and Murdoch [9] developed a surface elasticity theory for isotropic materials. In their model, the surface layer of a solid is treated as a membrane perfectly bonded to the material bulk. Lu et al. [10] modified the Gurtin-Murdoch model to develop a theory for modelling thin plates including surface effects. Surface energy effects on nanostructures have been studied by many researchers over the past decade. Bending properties of nanowires have been studied by Yun and Park [11] and Zhan et al. [12]. Liu and Rajapakse [13] presented closed-form solutions of static and free vibrating nanobeams under different boundary conditions considering surface stresses. Gheshlaghi and Hasheminejad [14] found exact solutions of the natural frequency of simply-supported nanobeams considering surface energy. Further, they used a dissipative surface stress model to study the effect size on natural frequencies of vibrating nanowires using Euler-Bernouli beam model [15] and Timoshenko beam model [16].

Since carbon nanotubes have significant waviness and curvature along the nanotubes length [17], it necessitates the consideration of curvature in the analysis of nano structures. Moreover, nanostructures can be exposed to different environmental and loading conditions, thus it is important to consider the effects of external thermal loads that may arise in such circumstances. In particular,

* Corresponding author.
E-mail address: mkhater@uwaterloo.ca (M.E. Khater).
Peer review under responsibility of Karabuk University.

http://dx.doi.org/10.1016/j.jestch.2014.07.003

the static stability of nanowires under thermal and mechanical loads is an important consideration since the wires undergo qualitatively large deformations once they undergo the pitch-fork bifurcation known commonly as buckling. Wang and Feng [18] studied the buckling of nanowires under uniaxial compression taking into account the effect of surface energy and residual surface tension. Wang and Yang [19] studied the effect of residual surface stress and surface elasticity on the post buckling state of nanowires under larger deflections using the shooting method.

Considering nonlocal elasticity, Mahmoud et al. [2] presented a static analysis of nanobeams including surface effects using the finite element method. Mohammadi et al. [17] studied the static instability of a curved nonlocal nanobeam on elastic foundation. Thongyothee and Chucheepsakul [20] investigated the post buckling of nanorods subjected to an end concentrated load, accounting for surface energy and nonlocal elasticity. They found that surface stress significantly increases structural stiffness and thus results in resisting post buckling load and end displacement. Lee and Chang [21] studied buckling of a cantilever nanowire with varying diameter considering surface effects and employing nonlocal elasticity. They found that the influence of surface effects on the critical buckling load is significant. Tounsi et al. [22,23] studied the thermal buckling of straight nanobeams where they employed a high-order beam theory using nonlocal elasticity. Further, using a nonlocal Timoshenko beam model, Semmah et al. [24] found that the critical buckling temperature is dependent on the chirality of zigzag carbon nanotubes.

To the knowledge of the authors, buckling analysis of curved nanowires under thermal loading and considering surfaces forces has not been addressed in literature. This work presents an effort towards investigating such conditions. In the present work, a model is developed to study the static buckling behavior of curved nanobeams under thermal loads, taking into account the surface effects. The beam is modelled as an Euler-Bernoulli beam with curvature, incorporating the surface constitutive relations of Gurtin and Murdoch. The mathematical model is presented in Section 2. Section 3 shows the results and parametric studies. Concluding remarks are then given in Section 4.

2. Model

Based on kinematic assumption of Euler-Bernoulli beam including nonlinear von Kármán strain (midplane stretching) and thermal strain, the axial strain of curved wire can be described by.

$$\varepsilon_{xx}=\frac{\partial u}{\partial x}+\frac{1}{2}\left(\frac{\partial w}{\partial x}\right)^2+\frac{\partial w}{\partial x}\frac{\partial w_0}{\partial x}-\alpha_{th}\Delta T-z\frac{\partial^2 w}{\partial x^2}=\varepsilon_0+zk_x \quad (1)$$

where u,w and w_0 are the axial displacement, transverse displacement, and initial rise of a generic point along the beam axis relative to the mid-plane. α_{th} and ΔT are, respectively, the thermal expansion coefficient of the nanowire and temperature difference between the wire and environment. The parametersε_0 and k_x are the longitudinal and bending strains, respectively, which are described by

$$\varepsilon_0=\frac{\partial u}{\partial x}+\frac{1}{2}\left(\frac{\partial w}{\partial x}\right)^2+\frac{\partial w}{\partial x}\frac{\partial w_0}{\partial x}-\alpha_{th}\Delta T \quad (2.a)$$

$$k_x=-\frac{\partial^2 w}{\partial x^2} \quad (2.b)$$

The force resultant N and bending moment resultant M due to normal stress σ_{xx} can be described as.

$$N=\int_A \sigma_{xx}\mathrm{d}A=EA\varepsilon_0 \quad (3.a)$$

$$M=\int_A z\sigma_{xx}\mathrm{d}A=EIk_x \quad (3.b)$$

where I is the second area moment,A is the cross sectional area, and E is Young's modulus. Using the principle of virtual displacement, we obtain

$$0=\int_0^L\left[(N\delta\varepsilon_0+M\delta k_x)-\left(q\delta w+f\delta u+\overline{P}\frac{\partial w}{\partial x}\frac{\partial \delta w}{\partial x}\right)\right]\mathrm{d}x \quad (4)$$

where q and f are transverse and axial distributed forces (measured per unit length), and $\overline{P}$ is an applied axial compressive force at the boundaries. Substituting Eq. (3) into Eq. (4), the following equilibrium equations can be derived:

$$\delta u:\frac{\partial N}{\partial x}+f=0 \quad (5.a)$$

$$\delta w:\frac{\partial}{\partial x}\left(N\frac{\partial w}{\partial x}\right)+\frac{\partial^2 M}{\partial x^2}+q-\overline{P}=0 \quad (5.b)$$

According to Gurtin-Murdoch model, the constitutive relations of the surface can be expressed as

$$\sigma_{xx}^s=\tau_0-\frac{\tau_0}{2}\left(\frac{\partial w}{\partial x}\right)^2+(2\mu_0+\lambda_0)\varepsilon_{xx}\quad \text{at } z=\pm\frac{h}{2} \quad (6.a)$$

$$\sigma_{xz}^s=\tau_0\frac{\partial w}{\partial x}\quad \text{at } z=\pm\frac{h}{2} \quad (6.b)$$

where τ_0 is the residual surface stress under no-load conditions, h is the thickness, andμ_0 and λ_0 are surface Lamé's constants, which can be determined from atomistic calculations. According to Euler beam theory, the stress componentσ_{zz} is small and thus neglected. However, σ_{zz} must be considered to satisfy the surface equilibrium which is assumed to vary linearly through the beam thickness [13]

$$\sigma_{zz}=\frac{2z\tau_0}{h}\frac{\partial^2 w}{\partial x^2} \quad (7)$$

Now, including the surface stress componentσ_{zz} of bulk stress of the nanobeam yields.

$$\sigma_{xx}=E\varepsilon_{xx}+\upsilon\sigma_{zz} \quad (8)$$

where E and υ are Young's modulus and Poisson's ratio, respectively.

Neglecting distributed axial and transverse forces q and f, the equilibrium equation of a clamped–clamped curved nanowire of length L including an axial force at the boundary $\overline{P}$, an axial thermal load, and surface stress effects can be described by [9,13]

$$\left[EI-\frac{2\upsilon I\tau_0}{h}+(2\mu_0+\lambda_0)I_s\right]\frac{\partial^4 w}{\partial x^4}+\left[\overline{P}+EA\alpha_{th}\Delta T-\pi r\tau_0-\frac{AE}{2L}\int_0^L\left(\left(\frac{\partial w}{\partial x}\right)^2+2\frac{\partial w}{\partial x}\frac{\partial w_0}{\partial x}\right)dx\right]\times\left(\frac{\partial^2 w}{\partial x^2}+\frac{\partial^2 w_0}{\partial x^2}\right)=0 \quad (9.a)$$

subject to the boundary conditions

$$w(x=0)=0,\quad \frac{\partial w(x=0)}{\partial x}=0,\quad w(x=L)=0,\quad \text{and}\quad \frac{\partial w(x=L)}{\partial x}=0 \tag{9.b}$$

where I_s is the surface moment of area. In case of a nanowire, $I_s=\pi r^3$ where r is the wire radius.

To generalize the results, we perform nondimensionlization by introducing the nondimensional variables

$$\widehat{x}=\frac{x}{L}\quad\text{and}\quad \widehat{w}=\frac{w}{r_g} \tag{10}$$

where r_g is the radius of gyration, $r_g=\sqrt{I/A}$. The nondimensional equilibrium equation takes the form

$$\left[1-\frac{2\upsilon\tau_0}{Eh}+\frac{(2\mu_0+\lambda_0)I_s}{EI}\right]\frac{\partial^4 w}{\partial x^4}+\left[P+N_{th}-\tau_s-\frac{1}{2}\int_0^1\left(\left(\frac{\partial w}{\partial x}\right)^2+2\frac{\partial w}{\partial x}\frac{\partial w_0}{\partial x}\right)dx\right]\times\left(\frac{\partial^2 w}{\partial x^2}+\frac{\partial^2 w_0}{\partial x^2}\right)=0 \tag{11.a}$$

subject to

$$w(x=0)=0,\quad \frac{\partial w(x=0)}{\partial x}=0,\quad w(x=1)=0,\quad \text{and}\quad \frac{\partial w(x=1)}{\partial x}=0 \tag{11.b}$$

where $P=\overline{P}L^2/EI$, $N_{th}=\alpha_{th}\Delta TL^2/r_g^2$, $\tau_s=\pi r\tau_0 L^2/EI$, and the hats were dropped for simplicity.

The initial curved wire shape, $w_0(x)$, is approximated by [25]

$$w_0(x)=\frac{1}{2}a(1-\cos 2\pi x\ ). \tag{12}$$

The parameter a quantifies the rise of the wire at its midspan due its initial curvature, where $a=H/r_g$, and H is the dimensional initial wire rise due to its curvature. The shape of the wire under axial force is similar to the initial shape of the curved wire; thus it is assumed as

$$\mathrm{w}(x)=\frac{1}{2}b(\ 1-\cos 2\pi x) \tag{13}$$

where b is the midspan displacement due to applied axial force, measured from the initial wire configuration. Substituting Eqs. (12) and (13) into (11) yields

$$aP+bP-\frac{1}{2}a^2b\pi^2-\frac{3}{4}ab^2\pi^2-\frac{1}{4}b^3\pi^2-(a+b)\tau_s-4b\pi^2\mathrm{E}_s+aN_{th}+bN_{th}=0 \tag{14}$$

where $E_s=1+4(2\mu_0+\lambda_0)-\tau_s\nu/Er$.

The onset of buckling occurs when two roots of Eq. (14) are equal, i.e., the discriminant of (14) equals zero. This can be used to determine the critical buckling loads, P_{cr}. Further, solving Eq. (14) for b gives the wire pre- and post-buckling deflections due to applied axial force P.

3. Results

Nanowires are susceptible to buckling under thermal and compressive loads. Buckling corresponds to the appearance of multiple wire rise values for the same axial load. The axial load at which buckling initiates is dubbed the critical buckling load. In this section, we study the static stability of imperfect nanowires under compressive and thermal loads.

Fig. 1 depicts the relation between the wire radius and the critical buckling load P_{crs} normalized with respect to the critical buckling load P_{cr0} when no surface stress is considered. We consider a silicon nanowire with the material properties: $E=107$ GPa, $\alpha_{th}=2.56\times10^{-6}\,K^{-1}$, $\tau_0=0.6056$ N/m, $\lambda_0=-4.494$ N/m, and $\mu_0=-2.778$ N/m [13]. As can be seen from the figure, critical buckling load ratio increases as the wire radius decreases. Specifically, results show that the normalized critical load does not veer significantly from unity except for wires with radius of 2 nm or less. However, as wire radius decreases below 2 nm, the normalized critical load ratio increases exponentially reaching 30 for a wire radius of 0.5 nm. We conclude that surface stress effects are significant only for silicon nanowires with a radius of 2 nm or less.

Inspection of the equilibrium equation, Eq. (11), shows that surface effects reduce the contribution of the bending term while increasing the contribution of the nonlinear mid-plane stretching term to the overall wire stiffness. Our results show that surface effects harden the response of silicon nanowires, indicating that their dominant contribution to beam stiffness comes through nonlinear mid-plane stretching.

To study the impact of surface effects on nanowire static stability, we consider a silicon nanowire of length $L=100$ nm, radius $r=1.5$ nm, and initial wire rise $H=3.75$ nm (equivalent to nondimensional rise $a=5$). The nanowire rise pre- and post-buckling is shown in Fig. 2 for three levels of residual surface stress τ_s. The solid lines represent stable equilibrium positions of the nanowire while dashed lines represent unstable ones. As compressive load increases P, the rise b of the nanowire increases. At buckling, multi rise values appear for the same axial load magnitude. The asymmetry in the curves is due to initial wire curvature. Fig. 2 shows that residual surface stress τ_s tends to decrease the wire rise because of its tensile nature. It also shows the critical buckling load increases with τ_s implying an increase in wire stiffness.

The effects of surface modulus E_s on wire rise and buckled configurations are illustrated in Fig. 3, where critical buckling load

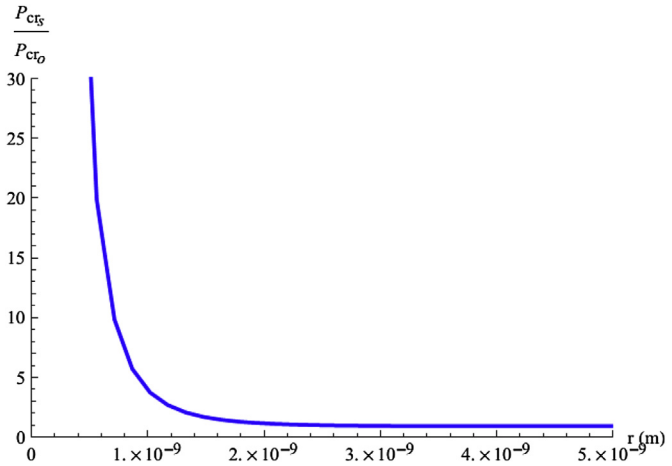

Fig. 1. The normalized critical buckling load as a function of wire radius for an initial rise of $a=5$ and thermal load $N_{th}=0$.

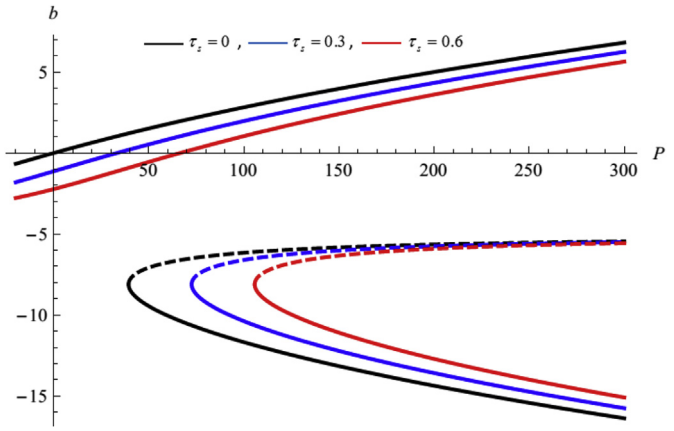

Fig. 2. Buckling configurations as functions of axial load P for three levels of residual surface stress τ_s, wire rise of $a = 5$, and thermal loads $N_{th} = 0$.

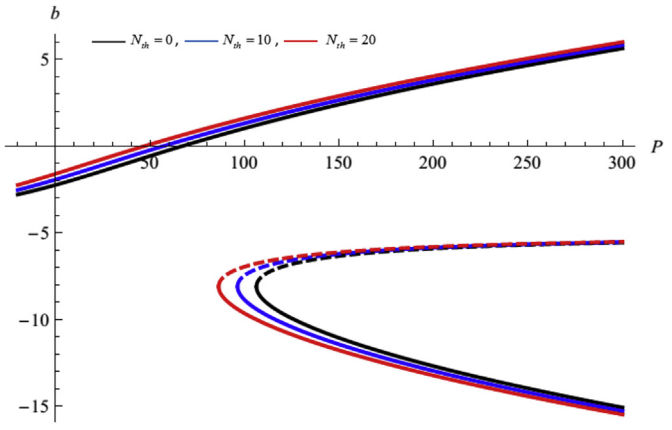

Fig. 4. Buckling configurations as a function of thermal load N_{th} at $a = 5$.

increases as the value of E_s increases from negative to positive highlighting the contribution of surface elasticity to bending stiffness. Large variations in wire rise are observed in the unstable and lower buckled configurations across the three magnitudes of the surface modulus E_s investigated. Since the surface modulus appears as a part of the linear bending term only, those variations indicate that the dominant contribution to wire stiffness for these equilibrium positions is due to the linear bending term. On the other hand, differences among the wire rise values for the three magnitudes of surface modulus E_s are insignificant for the upper buckled configuration indicating that the nonlinear mid-plane stretching term is the dominant contributor to beam stiffness in this case.

On the other hand, thermal loads affect all three buckled configurations consistently as seen in Fig. 4. The figure shows that the compressive critical buckling load decreases with increase in thermal load, which is expected due to the compressive nature of thermal loads.

We also investigate the relationship between wire curvature and buckling. Fig. 5 depicts the critical buckling load as a function of nondimensional wire rise a for three levels of tensile residual surface stress. It shows that the critical buckling load increases as tensile surface stress τ_s stiffens the wire. The results also provide estimates for the critical wire rise; this is the wire rise at which the axial load required for buckling switches from being compressive to tensile at $P_{cr} = 0$ [25]. Beyond the critical wire rise, the wire

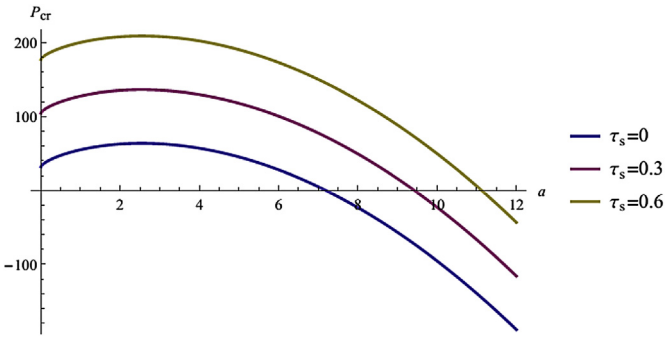

Fig. 5. The critical buckling load as a function of initial wire rise at three levels of residual surface stress.

collapses into one of the buckled positions even without the application of any compressive loads. In fact, the only way to maintain static stability of a wire with a rise larger than the critical rise is to apply to the wire a tensile axial load larger than P_{cr}. We find that increased tensile residual surface stress retards this process and increases the critical wire rise from 5.25 nm to 8.25 nm ($a = 7$ to $a = 11$).

We also investigated the relationship between wire curvature and buckling for different surface moduli E_s and different thermal loads N_{th}. We find that the critical buckling load and critical wire rise increase with increase in surface modulus, Fig. 6, due to increase in the surface resistance to bending. However, they decrease with thermal loads, Fig. 7, due to the compressive nature of thermal loads.

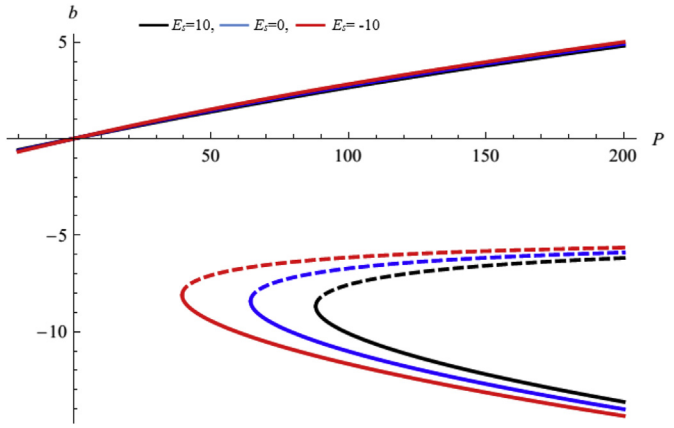

Fig. 3. Buckling configurations as a function of surface moduli E_s at $a = 5$, $N_{th} = 0$, and $\tau_s = 0$.

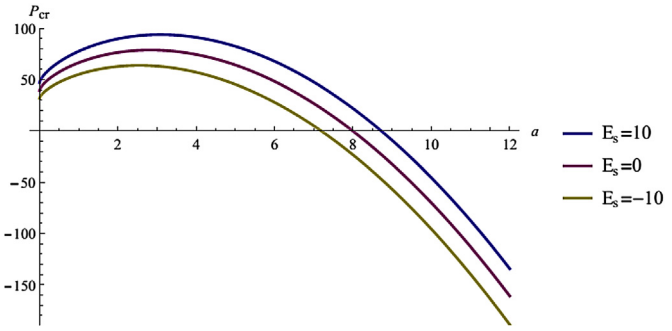

Fig. 6. The critical buckling load as a function of initial wire rise at three values of surface moduli and $\tau_s = 0$.

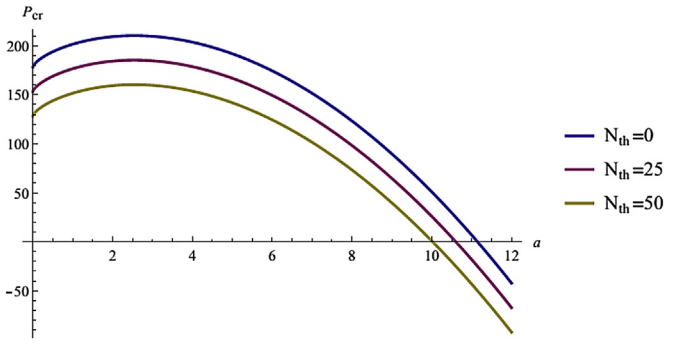

Fig. 7. The critical buckling load as a function of initial wire rise at three levels of thermal loads.

4. Conclusions

In this work, we developed the equilibrium equation for curved nanowires under axial and thermal loads taking into account surface energy effects. We used this equation to investigate the static stability and post-buckled configurations of those wires. The results show the relationships among nanowire curvature, axial and thermal loads, and surface energy and their impact on wire stability and post-buckling behavior. In particular, we report the buckled configurations, critical buckling loads, and critical rise of silicon nanowires.

Our analysis manifests the importance of surface energy to the response of silicon nanowires with a diameter less than 4 nm. It shows that the critical buckling load and critical wire rise increases with increase in tensile surface stress. Further, it shows that thermals decrease the critical buckling load and critical rise of nanowires.

References

[1] G. Yun, H. park, A multiscale, finite deformation formulation for surface stress effects on the coupled thermomechanical behavior of nanomaterials, Comput. Methods Appl. Mech. Eng. 197 (2008) 3337–3350.
[2] F. Mahmoud, M. Eltaher, A. Alshorbagy, E. Meletis, Static analysis of nanobeams including surface effects by nonlocal finite element, J. Mech. Sci. Technol. 26 (2012) 1–9.
[3] G. Jing, H. Duan, X. Sun, Z. Zhang, J. Xu, Y. Li, J. Wang, D. Yu, Surface effects on elastic properties of silver nanowires: contact atomic-force microscopy, Phys. Rev. B 73 (2006) 235409/1–235409/6.
[4] J. He, C. Lilley, Surface effect on the elastic behavior of static bending nanowires, Nano Lett. 8 (2008) 1798–1802.
[5] J. He, C. Lilley, Surface stress effect on bending resonance of nanowires with different boundary conditions, Appl. Phys. Lett. 93 (2008) 263108/1–263108/3.
[6] E. Wong, P. Sheehan, C. Lieber, Nanobeam mechanics: elasticity, strength, and toughness of nanorods and nanotubes, Science 277 (1997) 1971–1975.
[7] P. Poncharal, Z. Wang, D. Ugarte, W. de Heer, Electrostatic deflections and electromechanical resonances of carbon nanotubes, Science 283 (1999) 1513–1516.
[8] S. Cuenot, C. Fretigny, S. Demoustier-Champagne, B. Nysten, Surface tension effect on the mechanical properties of nanomaterials measured by atomic force microscopy, Phys. Rev. B 69 (2004) 165410/1–165410/5.
[9] M. Gurtin, A. Murdoch, A continuum theory of elastic material surfaces, Arch. Ration. Mech. Anal. 57 (1974) 291–323.
[10] P. Lu, H. Lee, C. Lu, J. O'Shea, Surface tension effect on the mechanical properties of nanomaterials measured by atomic force microscopy, Phys. Rev. B 72 (2005) 085405/1–085405/5.
[11] G. Yun, H. Park, Surface stress effects on the bending properties of FCC metal nanowires, Phys. Rev. B 79 (2009) 195421/1–195421/15.
[12] H. Zhan, Y. Gu, C. Yan, P. Yarlagadda, Bending properties of Ag nanowires with pre-existing surface defects, Comput. Mater. Sci. 81 (2014) 45–51.
[13] C. Liu, R. Rajapakse, Continuum models incorporating surface Energy for static and dynamic response of nanoscale beams, IEEE Trans. Nanotechnol. 9 (2010) 422–431.
[14] B. Gheshlaghi, S. Hasheminejad, Surface effects on nonlinear free vibration of nanobeams, Composites B 42 (2011) 934–937.
[15] S. Hasheminejad, B. Gheshlaghi, Dissipative surface stress effects on free vibrations of nanowires, Appl. Phys. Lett. 97 (2010) 253103/1–253103/3.
[16] B. Gheshlaghi, S. Hasheminejad, Size dependent surface dissipation in thick nanowires, Appl. Phys. Lett. 100 (2012) 263112/1–263112/4.
[17] H. Mohammadi, M. Mahzoon, M. Mohammadi, M. Mohammadi, Postbuckling instability of nonlinear nanobeam with geometric imperfection embedded in elastic foundation, Nonlinear Dyn. (2014) 1–12.
[18] G. Wang, X. Feng, Surface effects on buckling of nanowires under uniaxial compression, Appl. Phys. Lett. 94 (2009) 141913/1–141913/3.
[19] G. Wang, F. Yang, Postbuckling analysis of nanowires with surface effects, J. Appl. Phys. 109 (2011) 063535/1–063535/4.
[20] C. Thongyothee, S. Chucheepsakul, Postbuckling behaviors of nanorods including the effects of nonlocal elasticity theory and surface stress, J. Appl. Phys. 114 (2013) 243507/1–243507/7.
[21] H. Lee, W. Chang, Surface effects on axial buckling of nonuniform nanowires using non-local elasticity theory, Micro & Nano Lett. 6 (2011) 19–21.
[22] A. Tounsi, A. Semmah, A. Bousahla, Thermal buckling behavior of nanobeams using an efficient higher-order nonlocal beam theory, J. Nanomech. Micromech. 3 (2013) 37–42.
[23] A. Tounsi, S. Benguediab, E. Bedia, A. Semmah, M. Zidour, Nonlocal effects on thermal buckling properties of double-walled carbon nanotubes, Adv. Nano Res. 1 (2013) 1–11.
[24] A. Semmah, A. Tounsi, M. Zidour, H. Heireche, M. Naceri, Effect of chirality on critical buckling temperature of a zigzag single-walled carbon nanotubes using nonlocal continuum theory, Fullerenes, Nanotubes, Carbon Nanostruct. (2014).
[25] W. Lacarbonara, A Theoretical and Experimental Investigation of Nonlinear Vibrations of Buckled Beams, PhD thesis, Virginia Tech., Virginia, USA, 1997.